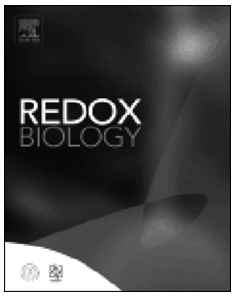

Molecular pathways driving omeprazole nephrotoxicity

Miguel Fontecha-Barriuso, Diego Martín-Sánchez, Julio M. Martinez-Moreno, Daniela Cardenas-Villacres, Susana Carrasco, Maria D. Sánchez-Niño, Marta Ruiz-Ortega, Alberto Ortiz, Ana B. Sanz

PII: S2213-2317(19)31607-6

DOI: https://doi.org/10.1016/j.redox.2020.101464

Reference: REDOX 101464

To appear in: *Redox Biology*

Received Date: 29 December 2019

Revised Date: 6 February 2020

Accepted Date: 11 February 2020

Please cite this article as: M. Fontecha-Barriuso, D. Martín-Sánchez, J.M. Martinez-Moreno, D. Cardenas-Villacres, S. Carrasco, M.D. Sánchez-Niño, M. Ruiz-Ortega, A. Ortiz, A.B. Sanz, Molecular pathways driving omeprazole nephrotoxicity, *Redox Biology* (2020), doi: https://doi.org/10.1016/j.redox.2020.101464.

Molecular pathways driving omeprazole nephrotoxicity

Miguel Fontecha-Barriuso BSc[1,2], Diego Martín-Sánchez BSc[1,2], Julio M. Martinez-Moreno PhD[1], Daniela Cardenas-Villacres BSc[1#], Susana Carrasco[1], Maria D. Sánchez-Niño PhD[1,2], Marta Ruiz-Ortega PhD[1,2,3], Alberto Ortiz PhD, MD, PhD[1,2,3,4], Ana B. Sanz PhD[1,2].

1. Research Institute-Fundacion Jimenez Diaz, Autonoma University, Madrid, Spain

2. REDINREN; Madrid, Spain

3. School of Medicine, UAM, Madrid, 28040, Spain

4. IRSIN, Madrid, 28040, Spain

Current address is Indian River Research and Educational Center, Department of Plant and Pathology, University of Florida, Fort Pierce, 34945, USA

Running tittle: Omeprazole and nephrotoxicity

Correspondence to:

Ana Belen Sanz, PhD

IIS-Fundacion Jimenez Diaz, Av Reyes Católicos 2, 28040 Madrid, Spain

Phone: +34 91.550.48.00, e-mail: asanz@fjd.es

or

Alberto Ortiz

IIS-Fundacion Jimenez Diaz, Av Reyes Católicos 2, 28040, Madrid, Spain

Phone: +34 91.550.48.00, e-mail: aortiz@fjd.es

Word count

Abstract: 237

Text: 4408

ABSTRACT

Omeprazole, a proton pump inhibitor used to treat peptic ulcer and gastroesophageal reflux disease, has been associated to chronic kidney disease and acute interstitial nephritis. However, whether omeprazole is toxic to renal cells is unknown. Omeprazole has a lethal effect over some cancer cells, and cell death is a key process in kidney disease. Thus, we evaluated the potential lethal effect of omeprazole over tubular cells.

Omeprazole induced dose-dependent cell death in human and murine proximal tubular cell lines and in human primary proximal tubular cell cultures. Increased cell death was observed at the high concentrations used in cancer cell studies and also at lower concentrations similar to those in peptic ulcer patient serum. Cell death induced by omeprazole had features of necrosis such as annexin V/7-AAD staining, LDH release, vacuolization and irregular chromatin condensation. Weak activation of caspase-3 was observed but inhibitors of caspases (zVAD), necroptosis (Necrostatin-1) or ferroptosis (Ferrostatin-1) did not prevent omeprazole-induced death. However, omeprazole promoted a strong oxidative stress response affecting mitochondria and lysosomes and the antioxidant N-acetyl-cysteine reduced oxidative stress and cell death. By contrast, iron overload increased cell death. An adaptive increase in the antiapoptotic protein BclxL failed to protect cells. In mice, parenteral omeprazole increased tubular cell death and the expression of NGAL and HO-1, markers of renal injury and oxidative stress, respectively.

In conclusion, omeprazole nephrotoxicity may be related to induction of oxidative stress and renal tubular cell death.

Key words: nephrotoxicity, omeprazole, oxidative stress, cell death, tubular proximal cells.

INTRODUCTION

The incidence of acute kidney injury (AKI) is approximately 2,000-3,000 per million population per year (1). AKI patients have a higher risk of developing chronic kidney disease (CKD) and end-stage renal disease (ESRD) (2). CKD is present in 10% of the adult population and is associated with an increased risk of AKI and premature mortality (3). AKI implies an abrupt decline in renal excretory function characterized by a reversible increase in the blood concentration of creatinine and other molecules, often associated with a decreased urine output (4, 5). Despite frequent recovery of renal function, mortality remains high, and even a short-timed injury contributes to a higher mortality (6). Tubular cell death is a common features of both AKI and CKD, eventually leading to tubulointerstitial fibrosis and progressive nephron loss (6). Both apoptosis and different pathways of regulated necrosis, such as necroptosis or ferroptosis, may contribute to tubular cell death (7-10).

Omeprazole is a proton pump inhibitor (PPI) prescribed to patients with gastroesophageal reflux disease and peptic ulcer. PPIs are among the most commonly prescribed drugs, although in a significant percentage of patients the prescription is not justified and self-medication is common (11). PPIs inhibit the H+/Na+ ATPase in gastric cells, thus decreasing proton secretion into the gastric lumen. Additionally, they also inhibit vacuolar ATPase (V-ATPase), and may have antiproliferative actions in tumor cells (12, 13). Thus, omeprazole inhibits pancreatic cancer cell growth (12, 13), and promotes apoptosis in human melanoma cells and in B-cell malignancies (12, 14). Omeprazole is a cause AKI due to acute tubulointerstitial nephritis (AIN), especially in the elderly (15-19). Additionally, two recent independent studies associated PPI consumption to an excess risk for CKD (20-23), and a recent prospective, double-blinded cohort study disclosed that omeprazole prophylaxis was associated to increased serum creatinine among patients admitted to hospital (24). However, the cellular and molecular mechanisms of PPI nephrotoxicity in general and specifically of omeprazole, have not been characterized, thus hampering prevention and therapy efforts.

METHODS

Cell and reagents

Three types of cells were studied, human (HK-2) (25) and murine (MCT) (26) immortalized proximal tubular epithelial cell lines, and primary human proximal tubular cell cultures (RPTEC, Cambrex, East Rutherford, NJ, USA). HK-2 cells were grown in RPMI 1640 (GIBCO), 10% decomplemented fetal bovine serum (FBS), 1% glutamine, 100 U/mL penicillin, 100 µg/mL streptomycin, 5 µg/mL Insulin Transferrin Selenium (ITS) and 36 ng/mL hydrocortisone in 5% CO_2 at 37 °C. MCTs were grown in RPMI 1640, 10% FBS, 100 µg/mL streptomycin, 2 mM glutamine and 100 U/mL penicillin. RPTEC were grown in REGM (renal epithelial cell growth medium; GIBCO). At 60–70% of confluence, cells were growth-arrested in serum-free medium for 24 hours before the experiments.

Omeprazole (Selleckchem, Munich, Germany) was dissolved in DMSO and stored at -80º C. Cells were stimulated with high omeprazole concentrations (300 µM) for 3h, 18h, 24h and/or 48h, and with low concentrations (15, 20 and 30 µM) for 7 days. Ferrostatin (Fer-1, Santa Cruz Biotechnology, Santa Cruz, CA, USA) was used at 40µM, Necrostatin-1 (Nec-1, Sigma-Aldrich, St. Louis, MO) at 30µM, z-VAD-fmk (Bachem, Bubendorf, Switzerland) at 100µM, and N-acetyl-cysteine (NAC, Sigma-Aldrich) at 1 mM concentrations, based on prior dose response-studies and experience inhibiting tubular cell death triggered by different stimuli (7). 3-methyladenine (3-MA, Sigma-Aldrich) was resuspended at 100 mM in distilled H_2O. Staurosporine at 500 nM (Sigma-Aldrich) was used as positive control for apoptosis and H_2O_2 (0.4mM) as positive control for reactive oxygen species (ROS) production. Peptide BclxL-BH4 (Merck, Darmstadt, Germany) was used at concentrations based on previous experience with the drug in cultured tubular cells (27).

Assessment of cell death

Cell viability was estimated using the 3-[4,5-dimethylthiazol-2-yI]-2,5 diphenyltetrazolium bromide (MTT, Sigma-Aldrich) colorimetric assay. Following stimulation,

culture medium was removed, and cells were incubated with 0.5 mg/mL MTT in PBS for 1h at 37 ºC. The resulting formazan crystals were dried and dissolved in DMSO. Absorbance (indicative of cell viability) was measured at 570 nm using a plate reader (TECAN infinite F200).

For assessment of cell death by annexin V/7-amino-actinomycin D (7-AAD) staining, 5 × 10^5 cells were washed with ice-cold PBS, resuspended in 100 µl binding buffer, and stained with 2.5 µl PE-Annexin V and 2.5 µl 7-AAD for 15 min at 37 °C in the dark. Then, 400 µl binding buffer was added just before flow cytometry. Cells were analyzed using FACS Canto cytometer and FACS Diva Software (BD Biosciences, Eysins, Switzerland). Early and late cell death was evaluated on PE fluorescence (Annexin V) versus PerCP (7-AAD) plots. Cells stained only with annexin V were considered early cell death; cells stained with both annexin V and 7-AAD were considered late cell death or necrosis.

Cytotoxicity was assessed by the release of lactate dehydrogenase (LDH) using the Cytotoxicity Detection Kit PLUS (LDH) according to the manufacturer's instructions (Roche). Fluorescence was recorded using a plate reader (TECAN infinite F200).

Nuclear morphology was assessed in formalin-fixed cells stained with DAPI (Sigma) and observed with fluorescence microscopy (Nikon E600). Cell morphology was further examined by transmission electron microscopy (TEM) in a Jeol Jem1010 (100Kv) microscope. Cells were fixed in 4% formaldehyde/2% glutaraldehyde in PBS, dehydrated and embedded in Epon resin.

Western Blot

Cells were homogenized in lysis buffer (50 mM TrisHCl, 150 mM NaCl, 2 mM EDTA, 2 mM EGTA, 0.2% Triton X-100, 0.3% NP-40, 1 mM PMSF and 1 µg/ml pepstatin A). Protein concentration was measured with the BCA (bicinchoninic acid) assay (Thermo Fisher, Waltham, MA). Equal amounts of protein were loaded in 15% SDS gel, separated by electrophoresis and transferred to PVDF membranes (polyvinylidene difluoride, Millipore, Darmstadt, Germany). The membranes were blocked with 5% TBS/0.5% v/v Tween-20 skim milk and incubated with anti-caspase3 (1:1000, Cell Signaling Technology, Danvers, MA), anti-

BcLxL (1:250, Santa Cruz), anti-Bax (1:100, BD Pharmingen, San Jose, CA), anti-LC3 (1:1000, Novus Bio, Centennial, CO) or anti-heme oxygenase (HO-1, 1:1000, Enzo Life Technologies, Farmigdale, NY) antibodies dissolved in 5% milk PBS/Tween for 1h at room temperature. They were then washed with TBS/Tween and incubated with the secondary antibodies against rabbit IgG (1:5000) or mouse IgG (1:5000). After washing with PBS/Tween, blots were developed with the chemiluminescence method (ECL; Thermo Fisher) and probed with mouse monoclonal anti–alpha-tubulin antibody (1:10000, Sigma-Aldrich). Levels of expression were corrected for minor differences in loading.

RNA extraction and real-time polymerase chain reaction

Total RNA was extracted by the TRI Reagent method (Invitrogen, Thermo Fisher) and 1 µg RNA was reverse transcribed with High Capacity cDNA Archive Kit (Applied Biosystem, Thermo Fisher) (28). Quantitative PCR was performed in a 7500 Real Time PCR System with the Prism 7000 System SDS Software using predeveloped primers (Thermo Fisher). RNA expression of different genes was corrected for GAPDH.

ROS production

To assess total ROS production, 2',7'-dichlorodihydrofluorescein diacetate CM-H2DCFDA (Molecular Probes, Thermo Fisher) was added 3 hours before flow cytometry. To assess lipid peroxidation, cells were washed and BODIPY 581=591 C11 (Invitrogen, Thermo Fisher) was added for 1h before flow cytometry. After staining, cells were trypsinized, washed and transferred to FACS tubes in RPMI containing 10% FBS. Mitochondrial ROS was measured with MitoSOX red mitochondrial superoxide indicator (Invitrogen, Thermo Fisher). After different treatments cells were incubated with 2.5 µM MitoSOX for 10 minutes at 37 ºC and then fluorescence was measured at 510/580 (Ex/Em) (Spire Multilabel Reader, Perkin Elmer, Waltham, MA).

NADPH activity

NADPH activity was measured by the lucigenin chemiluminescence assay as described (29). Renal cell homogenates in 50 mmol/L phosphate buffer containing 0.01 mmol/L EDTA, 0.32 mol/L sucrose and 0.1% protease inhibitor cocktail were transferred to Röhren tubes and then

5 μmol/L lucigenin and 100 μmol/L NADPH (Sigma-Aldrich) were added. Chemiluminiscence was measured with a luminometer (Berthold Technologies, Bad Wildbad, Germany) by counting the photon emission at 10-s intervals over 5–10 min and values were normalized over non-omeprazole stimulated tubular cells.

Clonogenic assays

Cells were pre-treated with NAC for 1 hour, and then stimulated with omeprazole. After 48 hours, cells were detached with trypsin-EDTA, seeded in Petri dishes and cultured in 10% FBS RPMI 1640 for 7 days. Then, they were fixed and stained with crystal violet. Petri dishes were photographed and cells were resuspended in ethanol: sodium citrate 1:1 (0.1 M, pH 4.2), and absorbance (indicative of colony formation) was measured at 570 nm (TECAN infinite F200).

Assessment of lysosomal acidity

The lysosomal function of cells was assessed using a lysosomotropic tracking dye called LysoTracker® Red DND-99 (Life Technologies, Thermo Fisher), which accumulates in lysosomes due to proton trapping (30). Cells were scraped into culture medium, collected into sterile polypropylene tubes and centrifuged at 500 x g for 5 min at room temperature to remove cell debris. Then LysoTracker Red (500 nM) was added in RPMI-1640 for 30 min at 37 °C and cells were washed twice with PBS resuspended in FACS buffer and analyzed using FACS Canto cytometer and FACS Diva Software (BD Biosciences).

Measurement of intracellular ATP concentration

ATP levels were measured by the Luminiscente ATP Detection Assay Kit (Abcam, Cambridge, UK) following the manufacturer´s instructions.

Animal model

All procedures were conducted in accordance with the NIH Guide for the Care and Use of Laboratory Animals and were approved by the animal ethics committee of IIS-FJD (PROEX 17/070). Wild-type 12-week-old female C57BL/6 mice received 40 mg/kg/day omeprazole (Normon, Madrid, Spain) or vehicle intraperitoneally for 10 or 28 days (4-5 animals per group). Dosing was based on human therapeutic dosing and its conversion to mice dosing following FDA guidelines, based on body surface area (31, 32), using the FDA dose range for omeprazole

(33) (**Fig. S1**). Thus, the murine dose was within the range of the murine equivalent dose. Blood was drawn to assess serum creatinine and blood urea nitrogen (BUN), and kidneys were perfused in situ with cold saline before removal. One kidney was snap-frozen in liquid nitrogen for RNA and protein studies and the other was fixed and paraffin embedded for histological studies.

TUNEL

Terminal deoxynucleotidyl transferase-mediated dUTP nick end labeling (TUNEL) assay was performed in 3 µm thick sections of paraffin-embedded tissue with the *In Situ* Cell Death Detection Kit, Fluorescein (Roche Applied Science, Penzberg, Germany), according to the manufacturer's instructions.

Statistics

Results are expressed as mean ± SEM. Differences between groups were evaluated using Q2 one-way ANOVA with Tukey's post-hoc tests using the Prism software (Graphpad 7.04). For pairs of samples, data were analyzed using non-parametric Mann–Whitney test. A p-value < 0.05 was considered statistically significant.

RESULTS

Omeprazole induces tubular cell death

First, the effect of omeprazole on proximal tubular cell viability was tested. Omeprazole decreased cell viability in murine tubular cells as assessed by MTT (**Fig. 1.A**). Moreover, omeprazole also decreases cell viability in both immortalized (HK-2) and primary cultures (RPTEC) of human proximal tubular cells (**Fig. 1.A**). The effect of omeprazole was dose-dependent and more evident at 48h than at 24h. HK-2 cells were studied in more detail. Phase contrast imaging showed cell detachment and morphological changes, such as vacuole formation, in response to omeprazole (**Fig. 1.B, C**).

The concentration (150-350 µM) of omeprazole in figures 1.A-C is similar to the concentration reported to induce tumor cell death (34). However, the omeprazole concentration in serum of patients on omeprazole is lower, around 20 µM (35). Thus, we tested the effect of lower concentrations of omeprazole for longer times of exposure. Omeprazole at 20 and 30 µM

for 7 days also decreased cell viability as assessed by MTT and induced cell detachment and vacuole formation (**Fig. 1.D, E**).

Characterization of omeprazole-induced tubular cell death

Next, we characterized the lethal effect of omeprazole on tubular cells. Cell death was assessed by annexin V/7-AAD staining (**Fig. 2.A**). Omeprazole increased the number of annexin V^+/7-AAD^+ cells in a dose- and time-dependent manner, while the number of annexin V^+/7-AAD^- cells did not change, suggesting that cell death could be mediated by necrosis, rather than by apoptosis (**Fig. 2.A**). The necrotic effect of omeprazole was confirmed by cytotoxicity assay measuring the release of LDH (36) (**Fig. 2.B**). Furthermore**,** nuclear morphology, analyzed by DAPI staining, showed irregular chromatin clumping typical of necrosis and ultrastructural analysis by TEM showed striking vacuole formation and plasma membrane rupture (**Fig. 2.C, D**). Previous reports have suggested that apoptosis could play a role in omeprazole-induced cell death (12), although the role of caspases has not been clarified (34). Therefore, to evaluate the role of apoptosis in omeprazole-induced tubular cell death, we tested caspase activation. A weak cleaved caspase 3 band was detected by western blot in tubular cells stimulated with omeprazole, but levels were lower than in cells stimulated with staurosporine, a positive control of apoptosis (37) (**Fig. S2.A**). Moreover, the pan-caspase inhibitor zVAD did not prevent omeprazole-induced cell death (**Fig. S2.B, C**). In recent years, new pathways of regulated necrosis, such as necroptosis or ferroptosis, have been shown to contribute to kidney disease (9, 38), thus we tested their contribution to omeprazole-induced tubular cell death. Pre-treatment with Necrostatin-1 (Nec-1) or Ferrostatin-1 (Fer-1), at concentrations previously shown to prevent necroptosis and ferroptosis respectively in tubular cells, was unable to prevent omeprazole-inducedcell death/loss of cell viability (**Fig. S2.B, C**).

Omeprazole-induced cell death is associated to increased ROS production

Based on a previous report of the association of omeprazole cytotoxicity with oxidative stress (12), we analyzed ROS production in HK-2 cells stimulated with omeprazole. Omeprazole 300 μM induced a strong and early increase in ROS production as assessed by CM-H2DCFDA staining and flow cytometry **(Fig. 3.A**). Moreover, lower concentrations of

omeprazole, similar to those found in the circulation of patients on omeprazole, also promoted a strong ROS production (**Fig. 3.B**). The mitochondria and NADPH oxidase are the major sources of intracellular ROS, so we analyzed their possible involvement in driving omeprazole-induced ROS accumulation. We measured mitochondrial ROS production by MitoSOX staining, observing that omeprazole promotes mitochondrial ROS (**Fig. 3.C**). In addition, we observed that omeprazole increased NADPH oxidase activity but this followed the increase in ROS production, suggesting that NADPH oxidase activity is not the initial or main driver of oxidative stress induced by omeprazole (**Fig 3. D**). Moreover, we observed by BODIPY staining and flow cytometry that increased ROS production was followed by lipid peroxidation at later time points (**Fig. 3.E**).

NAC prevents omeprazole-induced cell-death

Next, we tested the effect of the common ROS scavenger N-acetyl-cysteine (NAC) over oxidative stress and cell death induced by omeprazole in tubular cells. NAC prevented total and mitochondrial ROS production and lipid peroxidation induced by omeprazole (**Fig. 4.A-C**). Moreover, NAC prevented cell death induced by omeprazole as assessed by LDH release and by Annexin V/7-AAD staining, and also prevented cell detachment and vacuole formation (**Fig. 4.D-F**). In addition, clonogenic assays showed that cells exposed to omeprazole are unable to form colonies, but NAC reversed the decreased clonogenic survival, an observation consistent with increased cell survival (**Fig. S3**). Altogether, these results suggest that omeprazole-induced tubular cell death is initiated by a strong oxidative stress that leads to lipid peroxidation. Since lipid peroxidation and mitochondrial stress may trigger to other types of cell death such as ferroptosis or apoptosis, we explored the involvement of these forms of cell death in response to the initial wave of ROS production. To test this hypothesis, we pre-treated the cells with a combination of NAC and zVAD or Nec-1 or Fer-1, and we observed that protection from cell death was increased when NAC was combined with zVAD or Fer-1 (**Fig. 4.G**).

Omeprazole induces lysosomal alkalization and reduces ATP levels

Omeprazole alters intracellular pH in tumor cells. Thus, we analyzed the effect of omeprazole on lysosomal pH by detecting the fluorescence intensity of LysoTracker® Red

DND-99. We observed that omeprazole decreased the fluorescence intensity in HK-2 cells (**Fig. 5.A**), indicating an increase in lysosomal pH. Moreover, lysosomal alkalization was prevented with NAC (**Fig. 5.B**), suggesting that ROS production is an early event upstream of the altered intracellular pH gradients.

Next, we assessed intracellular ATP levels. In contrast breast cancer cells, where PPIs increased ATP levels and this was ascribed to inhibition of V-ATPase activity (39), we observed that omeprazole dramatically decreases intracellular ATP levels in tubular cells (**Fig. 5.C**). Intracellular ATP decreased at early times points and, as the increased ROS levels, it was already observed at 1 hour (**Fig. 5.C)**, suggesting that together with oxidative stress it may a driver of cell death. In this regard, the decrease in ATP production was little responsive to NAC (**Fig. 5.D**).

Omeprazole promotes expression of BclxL and autophagy in HK-2 cells

BclxL and Bax are members of Bcl-2 family proteins which regulate cell death at the mitochondrial level. Since omeprazole induced mitochondrial oxidative stress, we measured the BclxL/Bax ratio, observing that omeprazole upregulates the antiapoptotic protein BclxL while the levels of proapoptotic Bax were weakly downregulated, leading to an increased BclxL/Bax ratio (**Fig. 6.A, B**). This suggests that, similar to the response to other nephrotoxic agents (8), the increased BclxL expression may be an adaptive response, which is unable to prevent cell death. However, the BclxL mimetic BclxL-BH4 (27) was not protective (**Fig. 6.C**).

Omeprazole also promotes autophagy as a survival mechanism in melanoma cells. Now, we observed that omeprazole may induce autophagy in HK-2 cells since it increased the LC3II/LC3Iratio at 48 hours as assessed by LC3 western blot (**Fig 6.D**). However, the autophagy inhibitor 3-methyladenine (3-MA) reduced LC3II/LC3I ratio (**Fig. 6.D**), but did not significantly modify the lethal effect of omeprazole, suggesting that autophagy is not a key pathway in omeprazole-induced cell death (**Fig. 6.E**).

Omeprazole-induced cell death may be modified by environmental factors

In routine clinical practice, omeprazole is frequently prescribed in association with other potentially nephrotoxic drugs, including oral anticoagulants. These drugs have been associated

with a specific form of kidney injury termed anticoagulant associated nephropathy characterized by recurrent hematuria and proximal tubular cell iron overload (40-42). Thus, we explored the interaction between iron overload and omeprazole. Sublethal iron overloading resulted in a higher lethal effect of omeprazole in tubular cells (**Fig. S4**).

Omeprazole induces renal injury in vivo

To explore the in vivo relevance of the cell culture results, we tested the effect of omeprazole in vivo. Omeprazole was injected daily to healthy mice for 10 or 28 days. While omeprazole did not increase serum creatinine or urea, which is consistent with its well-known lack of severe nephrotoxic potential, as is evident from its widespread clinical use, kidney expression of the tubular cell injury marker NGAL was increased (**Fig. 7.A, B**), and an increased tubular cell deathwas observed by TUNEL staining (**Fig. 7.C**). In addition, omeprazole increased the expression of the oxidative stress marker Heme-Oxygenase-1 (HO-1) at the mRNA and protein levels (**Fig. 7.D, E**). These results support the hypothesis that omeprazole has nephrotoxic potential by promoting cell death and are consistent with its clinical association with CKD. However, the nephrotoxic potential is low and in mice was subclinical.

DISCUSSION

Recent clinical data point to a subtle nephrotoxic effect of omeprazole, but the cellular and molecular mechanisms are unknown. Now, we have observed that omeprazole directly induces cell death in cultured tubular renal cells in vivo e in vitro through the generation of oxidative stress-induced cell death. Overall the data are consistent with omeprazole induced mitochondrial injury resulting in decreased ATP availability and increased oxidative stress, the latter driving cell death. Furthermore, these experiments have identified NAC as a potential nephroprotective drug in this context.

Omeprazole is one of the most widely used PPIs and prescription has increased significantly in recent years. However, in up to 40% of cases, PPI prescription does not follow the indications acknowledged by health authorities and, in some cases treatment is continued long term, regardless of clinical indication (43). This is an economic burden to healthcare systems as well as a risky practice, since long-term use of PPIs has been associated with

different adverse effects including AKI and CKD (44). Indeed, PPIs are frequently included in lists of drugs that are potential targets of deprescription strategies. When PPIs are appropriately prescribed, their benefits are likely to compensate their risks (45). However, a false sense of safety may have contributed to PPI abuse.

The first case of omeprazole-induced AIN was published in 1999 (46), and by 2009 there were 114 reported cases of PPIs-induced AIN (16). PPIs were a major cause of AIN in the elderly (18). Morerecent studies have identified PPIs as a risk factor for CKD, and higher doses of PPIs were associated with a higher risk of CKD (20-23). Moreover, a prospective study concluded that prophylaxis with omeprazole may contribute to renal impairment in males (24). Renal biopsies of omeprazole-induced AIN showed acute tubulitis and tubular infiltrates, while glomeruli were not injured (47). While the molecular mechanisms of injury may differ between AIN and CKD, this data suggest that tubular cells may be involved in at least some forms of omeprazole nephrotoxicity. Furthermore, the V-ATPase, a cellular target of PPIs, has key functions in tubular cells. Mutations in genes encoding the distal tubular V-ATPase cause genetic forms of distal tubular acidosis (48). More recently dysfunction of the proximal tubular V-ATPase, which has a different subunit composition from distal tubular V-ATPase, has been involved in Dent´s disease, characterized by proximal tubular cell injury and progressive CKD (49). Understanding the molecular and cellular mechanism of nephrotoxicity would support the biological plausibility of the PPI-kidney injury link and help develop preventive and therapeutic strategies.

We have now identified for the first time and characterized the molecular mechanisms of omeprazole-induced oxidative stress and cell death in tubular renal cells. Omeprazole-induced cell death had previously been observed in cancer cells and leukocytes (12-14, 34, 50). However, the cell death pathways activated by omeprazole may be cell type-dependent. In normal human lymphocytes omeprazole-induced cell death is mediated by apoptosis, while in human B-cell tumors cell death is caspase-independent (12, 50). We have observed that omeprazole promotes mild caspase-3 activation in tubular cells, but apoptosis did not trigger eventual cell death, since the pan-caspase inhibitor zVAD was not protective. Additionally,

neither necroptosis nor ferroptosis mediate cell death induced by omeprazole. However, morphological and functional characterization of tubular cell death induced by omeprazole showed features of necrosis such as early membrane permeabilization as assessed by Annexin V/7-AAD staining, LDH release, irregular chromatin condensation and presence of vacuoles. Omeprazole toxicity had been linked to oxidative stress in non-renal cells (12, 14, 51). In this regard, we have observed that omeprazole promotes a strong oxidative stress which was prevented by NAC suggesting that the main source of ROS is cytosolic. NOX4, a member of the NADPH oxidase, is the main source of cytosolic ROS in kidneys and contributes to different forms of renal disease (52). In melanoma cells omeprazole-induced oxidative stress is mediated by NADPH oxidase (14). However, omeprazole-induced NADPH oxidase activation in tubular cells occurred later that ROS production, thus, further studies are necessary to confirm the role of NOX4 in oxidative stress induced by omeprazole in tubular cells. In addition, omeprazole also induces mitochondrial ROS production at early time-points, which together with a dramatic decrease in ATP production may point to a key role of mitochondrial injury. V-ATPases are targets of omeprazole, and this or the decrease in ATP availability can explain the lysosomal alkalization observed in HK-2 cells. However, lysosomal alkalization seems to be a consequence of ROS production since it was prevented by NAC.

Different pathways of cell death potentially involved in renal injury include apoptosis, regulated necrosis (e,g, necroptosis or ferroptosis), as well as other forms of necrotic cell death that do not easily fit into one of these categories, like that induced by deferasirox in proximal tubular cells leading to deferasirox nephrotoxicity (8, 53). However, neither the RIPK1 specific inhibitor necrostatin-1 that prevents bona fide necroptosis in tubular cells and the kidney (7) nor the ferroptosis inhibitor ferrostatin-1 did, by themselves, prevent omeprazole-induced cell death. This suggests that omeprazole-induced cell death, despite being necrotic in nature, according to microscopical features, annexin V/7-AAD staining and LDH release, was not mediated by the two main forms of regulated necrosis (necroptosis and ferroptosis). However, our data are consistent with a model in which a strong oxidative stress will trigger necrosis, but a reduction of oxidative stress, as in the presence of NAC, will rescue some cells from this necrotic cell

death, but additional cell death pathways may be then activated and contribute to residual NAC-resistant cell death. Thus, in presence of NAC, both apoptosis and regulated necrosis through ferroptosis appear to be recruited, since the combination of NAC with Fer-1 or the pan-caspase inhibitor zVAD offered additional protection. In this regard, the conversion from one form of cell death to another in presence of cell death inhibitors is not unusual. As an example, a cytokine cocktail composed of TWEAK, TNF and interferon-gamma elicits apoptosis in tubular cells, but when apoptosis is inhibited by zVAD, necroptotic cell death sensitive to necrostatin-1 is triggered and the number of dying cells increases (9, 37).

We also observed an increased mitochondrial stress under omeprazole, as well as increased levels of the anti-apoptotic protein BclxL. Increased expression of BclxL has been also observed in nephrotoxic AKI and thought to represent an adaptive nephroprotective mechanism (54). However, these higher BclxL levels or even higher levels following treatment with a BclxL mimetic were unable to prevent omeprazole nephrotoxicity. Likewise, autophagy can sometimes be activated as protective mechanism and, in this case, its inhibitor 3-MA may amplify the lethal effect, as observed for melanoma cells, where autophagy is an adaptive survival mechanism against drug-induced cytotoxicity including PPI (14). However, for tubular cells, no statistically significant impact of 3-MA was observed.

Omeprazole induced cell death in both murine and human tubular cells at concentrations found in serum of patients, supporting biological plausibility. In this regard, in vivo omeprazole also caused tubular cell injury, although only sensitive markers of kidney injury were altered, consistent with a low nephrotoxic potential and with clinical practice experience.

This study has several limitations that should be addressed in further studies. We have only explored the effect of omeprazole, but more PPIs are used in the clinic. Further studies should characterize the nephrotoxic potential of different PPIs. Furthermore, the in vivo dose of omeprazole was high. However, the in vivo data should be considered proof-of-concept and they were generated in young healthy mice, while PPIs are frequently used in elderly individuals with multiple comorbidities and using multiple prescription and over-the-counter

drugs with nephrotoxic potential, including non-steroidal anti-inflammatory agents, paracetamol and anticoagulants, among others (55-57). Additionally, omeprazole has been used at doses of up to 360 mg/day (33) and liver metabolism is saturable and decreases with repeating dosing, potentially leading to higher serum concentrations (https://www.accessdata.fda.gov/drugsatfda_docs/label/2012/019810s096lbl.pdf; accessed 23 December 2019).

Despite these limitations, this study strongly supports a direct toxic effect of omeprazole on tubular cells, and this was observed in cultured immortalized murine and human cells, and in primary cultures of human cells at clinically relevant concentrations and in vivo in mice. In this regard, anticoagulant-associated nephropathy is characterized by hematuria and proximal tubular cell iron overload (40, 42) and anticoagulated elderly individuals are frequently prescribed PPIs. Cell culture data suggest that the combination of omeprazole and iron overload may increase omeprazole nephrotoxicity. Additional comorbidities might impact omeprazole nephrotoxicity. Thus, in liver disease, plasma clearance of omeprazole is decreased by approximately 10-fold (https://www.accessdata.fda.gov/drugsatfda_docs/label/2012/019810s096lbl.pdf; accessed 23 December 2019).

In conclusion, we have shown for the first time, that omeprazole has a direct lethal effect over human tubular cells and have characterized some molecular pathways involved (**Fig. 8**). Omeprazole-induced cell death is caspase-independent, and ferroptosis and necroptosis are not involved. However, oxidative stress was evident and an antioxidant was protective. These findings lend biological plausibility to the epidemiological data linking PPIs to CKD and provide a basic framework for the development of less toxic PPIs as well as novel preventive and therapeutic strategies.

AUTHOR CONTRIBUTIONS

M.F.-B., A.O., and A.B.S. designed research; M.F.-B., D.M.-S., S.C., and JMM-M. performed research; M.F.-B., JMM-M, A.O., and A.B.S. analyzed data, A.O., and A.B.S. wrote the paper.

MDS-N and M.R-O. drafted and revised the paper; all authors approved the final version of the manuscript.

Acknowledgments. Supported by FIS CP12/03262, CP14/00133, PI16/02057, PI16/01900, PI18/01366, PI19/00588, PI19/00815, DTS18/00032, ERA-PerMed-JTC2018 (KIDNEY ATTACK AC18/00064 and PERSTIGAN AC18/00071, ISCIII-RETIC REDinREN RD016/0009 FEDER funds, Sociedad Española de Nefrología, Fundacion Renal IñigoÁlvarez de Toledo (FRIAT), ISCIII Miguel Servet (ABS, MDS-N), ISCIII Sara Borrell (JMM-M), , Comunidad de Madrid CIFRA2 B2017/BMD-3686 (MF-B and DM-S). No financial conflict of interest exists.

REFERENCES

1. Colpaert K, Hoste EA. Acute kidney injury in burns: a story of volume and inflammation. Crit Care. 2008;12(6):192.

2. Chawla LS, Kimmel PL. Acute kidney injury and chronic kidney disease: an integrated clinical syndrome. Kidney Int. 2012;82(5):516-24.

3. Kidney Disease: Improving Global Outcomes (KDIGO) CKD Work Group. KDIGO 2012 Clinical Practice Guideline for the Evaluation and Management of Chronic Kidney Disease. Kidney inter., Suppl. 2013; 3: 1–150

4. Wahab A, Saqladi AM. Acute kidney injury: New definitions and beyond. Journal of nephrology & therapeutics. 2016:1-4.

5. Kidney Disease: Improving Global Outcomes (KDIGO) Acute Kidney Injury Work Group. KDIGO Clinical Practice Guideline for Acute Kidney Injury. Kidney inter., Suppl. 2012; 2: 1–138.

6. Bellomo R, Kellum JA, Ronco C. Acute kidney injury. Lancet. 2012;380(9843):756-66.

7. Martin-Sanchez D, Fontecha-Barriuso M, Carrasco S, Sanchez-Niño MD, Mässenhausen AV, Linkermann A, et al. TWEAK and RIPK1 mediate a second wave of cell death during AKI. Proc Natl Acad Sci U S A. 2018;115(16):4182-7.

8. Martin-Sanchez D, Gallegos-Villalobos A, Fontecha-Barriuso M, Carrasco S, Sanchez-Niño MD, Lopez-Hernandez FJ, et al. Deferasirox-induced iron depletion promotes BclxL downregulation and death of proximal tubular cells. Sci Rep. 2017;7:41510.

9. Linkermann A, Braesen JH, Darding M, Jin MK, Sanz AB, Heller J-O, et al. Two independent pathways of regulated necrosis mediate ischemia-reperfusion injury. Proceedings of the National Academy of Sciences of the United States of America. 2013;110(29):12024-9.

10. Linkermann A, Skouta R, Himmerkus N, Mulay SR, Dewitz C, De Zen F, et al. Synchronized renal tubular cell death involves ferroptosis. Proc Natl Acad Sci U S A. 2014;111(47):16836-41.

11. Castillón F, Jiménez G, M, Dutres D, Moreno López A, González García L. Study of the use of omeprazole in a community pharmacy on the coast of girona. Biblioteca virtual en salud. 2010.

12. De Milito A, Iessi E, Logozzi M, Lozupone F, Spada M, Marino ML, et al. Proton pump inhibitors induce apoptosis of human B-cell tumors through a caspase-independent mechanism involving reactive oxygen species. Cancer Res. 2007;67(11):5408-17.

13. Udelnow A, Kreyes A, Ellinger S, Landfester K, Walther P, Klapperstueck T, et al. Omeprazole inhibits proliferation and modulates autophagy in pancreatic cancer cells. PLoS One. 2011;6(5):e20143.

14. Marino ML, Fais S, Djavaheri-Mergny M, Villa A, Meschini S, Lozupone F, et al. Proton pump inhibition induces autophagy as a survival mechanism following oxidative stress in human melanoma cells. Cell Death Dis. 2010;1:e87.

15. Torlot FJ, Whitehead DJ. Acute interstitial nephritis caused by two different proton pump inhibitors. Br J Hosp Med (Lond). 2016;77(1):50-1.

16. Ni N, Moeckel GW, Kumar C. Late-onset omeprazole-associated acute interstitial nephritis. J Am Geriatr Soc. 2010;58(12):2443-4.

17. Brewster UC, Perazella MA. Acute kidney injury following proton pump inhibitor therapy. Kidney Int. 2007;71(6):589-93.

18. Muriithi AK, Leung N, Valeri AM, Cornell LD, Sethi S, Fidler ME, et al. Clinical characteristics, causes and outcomes of acute interstitial nephritis in the elderly. Kidney Int. 2015;87(2):458-64.

19. Nadri Q, Althaf MM. Granulomatous tubulointerstitial nephritis secondary to omeprazole. BMJ Case Rep. 2014;2014.

20. Lazarus B, Chen Y, Wilson FP, Sang Y, Chang AR, Coresh J, et al. Proton Pump Inhibitor Use and the Risk of Chronic Kidney Disease. JAMA Intern Med. 2016;176(2):238-46.

21. Xie Y, Bowe B, Li T, Xian H, Yan Y, Al-Aly Z. Long-term kidney outcomes among users of proton pump inhibitors without intervening acute kidney injury. Kidney Int. 2017;91(6):1482-94.

22. Xie Y, Bowe B, Li T, Xian H, Balasubramanian S, Al-Aly Z. Proton Pump Inhibitors and Risk of Incident CKD and Progression to ESRD. J Am Soc Nephrol. 2016;27(10):3153-63.

23. Klatte DCF, Gasparini A, Xu H, de Deco P, Trevisan M, Johansson ALV, et al. Association Between Proton Pump Inhibitor Use and Risk of Progression of Chronic Kidney Disease. Gastroenterology. 2017;153(3):702-10.

24. Varallo FR, de Nadai TR, de Oliveira ARA, Mastroianni PC. Potential Adverse Drug Events and Nephrotoxicity Related to Prophylaxis With Omeprazole for Digestive Disorders: A Prospective Cohort Study. Clin Ther. 2018;40(6):973-82.

25. Poveda J, Sanchez-Niño MD, Glorieux G, Sanz AB, Egido J, Vanholder R, et al. p-cresyl sulphate has pro-inflammatory and cytotoxic actions on human proximal tubular epithelial cells. Nephrol Dial Transplant. 2014;29(1):56-64.

26. Haverty TP, Kelly CJ, Hines WH, Amenta PS, Watanabe M, Harper RA, et al. Characterization of a renal tubular epithelial cell line which secretes the autologous target antigen of autoimmune experimental interstitial nephritis. J Cell Biol. 1988;107(4):1359-68.

27. Santamaría B, Benito-Martin A, Ucero AC, Reyero A, Selgas R, Ruiz-Ortega M, et al. Bcl-xL prevents peritoneal dialysis solution-induced leukocyte apoptosis. Perit Dial Int. 2008;28 Suppl 5:S48-52.

28. Fontecha-Barriuso M, Martín-Sánchez D, Martinez-Moreno JM, Carrasco S, Ruiz-Andrés O, Monsalve M, et al. PGC-1α deficiency causes spontaneous kidney inflammation and increases the severity of nephrotoxic AKI. J Pathol. 2019;249(1):65-78.

29. Lopez-Sanz L, Bernal S, Recio C, Lazaro I, Oguiza A, Melgar A, et al. SOCS1-targeted therapy ameliorates renal and vascular oxidative stress in diabetes via STAT1 and PI3K inhibition. Lab Invest. 2018;98(10):1276-90.

30. Pierzyńska-Mach A, Janowski PA, Dobrucki JW. Evaluation of acridine orange, LysoTracker Red, and quinacrine as fluorescent probes for long-term tracking of acidic vesicles. Cytometry A. 2014;85(8):729-37.

31. Nair AB, Jacob S. A simple practice guide for dose conversion between animals and human. J Basic Clin Pharm. 2016;7(2):27-31.

32. USFDA. Guidance for Industry: Estimating the Maximum Safe Starting Dose in Adult Healthy Volunteer. Rockville, MD: US Food and Drug Administration; 2005, available at https://www.fda.gov/media/72309/download; accessed January 31, 2020

33. Prilosec® (omeprazole) delayed-release capsules; available at https://www.accessdata.fda.gov/drugsatfda_docs/label/2006/019810s083lbl.pdf; accessed January 31, 2020

34. Patlolla JM, Zhang Y, Li Q, Steele VE, Rao CV. Anti-carcinogenic properties of omeprazole against human colon cancer cells and azoxymethane-induced colonic aberrant crypt foci formation in rats. Int J Oncol. 2012;40(1):170-5.

35. Piqué JM, Feu F, de Prada G, Röhss K, Hasselgren G. Pharmacokinetics of omeprazole given by continuous intravenous infusion to patients with varying degrees of hepatic dysfunction. Clin Pharmacokinet. 2002;41(12):999-1004.

36. Chan FK, Moriwaki K, De Rosa MJ. Detection of necrosis by release of lactate dehydrogenase activity. Methods Mol Biol. 2013;979:65-70.

37. Justo P, Sanz AB, Sanchez-Niño MD, Winkles JA, Lorz C, Egido J, et al. Cytokine cooperation in renal tubular cell injury: the role of TWEAK. Kidney Int. 2006;70(10):1750-8.

38. Martin-Sanchez D, Ruiz-Andres O, Poveda J, Carrasco S, Cannata-Ortiz P, Sanchez-Niño MD, et al. Ferroptosis, but Not Necroptosis, Is Important in Nephrotoxic Folic Acid-Induced AKI. J Am Soc Nephrol. 2017;28(1):218-29.

39. Zhang S, Wang Y, Li SJ. Lansoprazole induces apoptosis of breast cancer cells through inhibition of intracellular proton extrusion. Biochem Biophys Res Commun. 2014;448(4):424-9.

40. Moreno JA, Martín-Cleary C, Gutiérrez E, Toldos O, Blanco-Colio LM, Praga M, et al. AKI associated with macroscopic glomerular hematuria: clinical and pathophysiologic consequences. Clin J Am Soc Nephrol. 2012;7(1):175-84.

41. de Aquino Moura KB, Behrens PMP, Pirolli R, Sauer A, Melamed D, Veronese FV, et al. Anticoagulant-related nephropathy: systematic review and meta-analysis. Clin Kidney J. 2019;12(3):400-7.

42. Brodsky SV, Satoskar A, Chen J, Nadasdy G, Eagen JW, Hamirani M, et al. Acute kidney injury during warfarin therapy associated with obstructive tubular red blood cell casts: a report of 9 cases. Am J Kidney Dis. 2009;54(6):1121-6.

43. Grant K, Al-Adhami N, Tordoff J, Livesey J, Barbezat G, Reith D. Continuation of proton pump inhibitors from hospital to community. Pharm World Sci. 2006;28(4):189-93.

44. Wilhelm SM, Rjater RG, Kale-Pradhan PB. Perils and pitfalls of long-term effects of proton pump inhibitors. Expert Rev Clin Pharmacol. 2013;6(4):443-51.

45. Freedberg DE, Kim LS, Yang YX. The Risks and Benefits of Long-term Use of Proton Pump Inhibitors: Expert Review and Best Practice Advice From the American Gastroenterological Association. Gastroenterology. 2017;152(4):706-15.

46. Ruffenach SJ, Siskind MS, Lien YH. Acute interstitial nephritis due to omeprazole. Am J Med. 1992;93(4):472-3.

47. Berney-Meyer L, Hung N, Slatter T, Schollum JB, Kitching AR, Walker RJ. Omeprazole-induced acute interstitial nephritis: a possible Th1-Th17-mediated injury? Nephrology (Carlton). 2014;19(6):359-65.

48. Fuster DG, Moe OW. Incomplete Distal Renal Tubular Acidosis and Kidney Stones. Adv Chronic Kidney Dis. 2018;25(4):366-74.

49. Satoh N, Yamada H, Yamazaki O, Suzuki M, Nakamura M, Suzuki A, et al. A pure chloride channel mutant of CLC-5 causes Dent's disease via insufficient V-ATPase activation. Pflugers Arch. 2016;468(7):1183-96.

50. Capodicasa E, Cornacchione P, Natalini B, Bartoli A, Coaccioli S, Marconi P, et al. Omeprazole induces apoptosis in normal human polymorphonuclear leucocytes. Int J Immunopathol Pharmacol. 2008;21(1):73-85.

51. Pinheiro LC, Oliveira-Paula GH, Portella RL, Guimarães DA, de Angelis CD, Tanus-Santos JE. Omeprazole impairs vascular redox biology and causes xanthine oxidoreductase-mediated endothelial dysfunction. Redox Biol. 2016;9:134-43.

52. Sedeek M, Nasrallah R, Touyz RM, Hébert RL. NADPH oxidases, reactive oxygen species, and the kidney: friend and foe. J Am Soc Nephrol. 2013;24(10):1512-8.

53. Martin-Sanchez D, Poveda J, Fontecha-Barriuso M, Ruiz-Andres O, Sanchez-Niño MD, Ruiz-Ortega M, et al. Targeting of regulated necrosis in kidney disease. Nefrologia. 2018;38(2):125-35.

54. Ortiz A, Lorz C, Catalán MP, Danoff TM, Yamasaki Y, Egido J, et al. Expression of apoptosis regulatory proteins in tubular epithelium stressed in culture or following acute renal failure. Kidney Int. 2000;57(3):969-81.

55. Fored CM, Ejerblad E, Lindblad P, Fryzek JP, Dickman PW, Signorello LB, et al. Acetaminophen, aspirin, and chronic renal failure. N Engl J Med. 2001;345(25):1801-8.

56. Perneger TV, Whelton PK, Klag MJ. Risk of kidney failure associated with the use of acetaminophen, aspirin, and nonsteroidal antiinflammatory drugs. N Engl J Med. 1994;331(25):1675-9.

57. Brodsky SV, Nadasdy T, Rovin BH, Satoskar AA, Nadasdy GM, Wu HM, et al. Warfarin-related nephropathy occurs in patients with and without chronic kidney disease and is associated with an increased mortality rate. Kidney Int. 2011;80(2):181-9.

LEGENDS OF FIGURES

Figure 1. Omeprazole induces cell death of both human and murine tubular cells. A) Murine (MCT) and human (HK-2 and RPTEC) tubular cells were exposed to different concentrations of omeprazole for 24h and 48h and cell viability was assessed by the MTT assay. Mean ± SD of three experiments *p<0.05 vs vehicle; **p<0.01 vs control; ***p<0.001 vs control. **B)** Time-course of omeprazole-induced cell death in HK-2 cells stimulated with 300 µM omeprazole. Mean ± SD of three experiments ***p<0.001 vs control. **C)** Phase contrast imaging of HK-2 cells stimulated with omeprazole. Magnification x200 (scale 100 µm) and detail x400 (scale 50 µm). Representative images of three experiments. **D, E)** HK-2 cells stimulated with low dose omeprazole for 7 days. **(D)** Cell viability Mean ± SD of five independent experiment; *p<0.05 vs control; ***p<0.001 vs control. **(E)** Representative images of three experiments. Magnification x200 (scale 100 µm) and detail x400 (scale 50 µm).

Figure 2. Omeprazole-induced cell death has features of necrosis. A) HK-2 cells were exposed to omeprazole for 24h, stained with annexin V/7-AAD and analyzed by flow cytometry. Omeprazole increased annexin V^+/7-AAD^+ cells but not annexin V^+/7-AAD^- cells. Mean ± SD of three independent experiments. **B**) Time-course of omeprazole-induced necrosis measured by LDH release. Mean ± SD of three independent experiment; **p<0.01 vs control; ***p<0.001 vs control. **C**) DAPI-stained cells exposed to 300 µM omeprazole for 24 hours disclosed irregular chromatin clumping suggestive of necrosis (arrow). Representative images of three independent experiments. Magnification x200 (scale 100 µm) and detail x400 (scale 50 µm). **D)** TEM of cells exposed to 300 µM omeprazole for 24 and 48 hours disclosed cells with a typical necrotic morphology, characterized by membrane rupture (add arrowhead) and extensive vacuolization (add arrow).

Figure 3. Omeprazole induced ROS production. HK-2 cells were stimulated with 300µM omeprazole (A, C-E) or lower concentrations (B) for different time periods. **A, B)** ROS production was assessed by CM-H2DCFDA staining and flow cytometry. Mean ± SD of four or three independent experiments. *p<0.05 vs control; **p<0.01 vs control; ***p<0.001 vs

control. **C)** Mitochondrial ROS production assessed by MitoSOX staining and flow cytometry. Mean ± SD of five independent experiments. *p<0.05 vs control; **p<0.01 vs control; ***p<0.001 vs control. **D)** NADPH oxidase activity was assessed by lucigenin chemiluminescence assay. Mean ± SD of three independent experiments. *p<0.05 vs control. **E**) Lipid peroxidation was assessed using the redox-sensitive dye BODIPY/581/591 C11. Mean ± SD of three independent experiments. *p<0.05 vs control; **p<0.01 vs control.

Figure 4. Omeprazole-induced cell death is ROS-dependent. HK-2 cells pretreated with 1 mM NAC for 1 hour and stimulated with 300 µM omeprazole for the indicated periods of time. **A-C)** ROS production, mitochondrial ROS and lipid peroxidation were measured at 24 hours. Mean ± SD of three of four independent experiments**.** **p<0.01 vs control; ***p<0.001 vs control; ##p<0.01 vs omeprazole; ###p<0.001 vs omeprazole. **D)** Necrosis was assessed by the LDH release assay. Mean ± SD of 4 independent experiments. ***p<0.001 vs control; ##p<0.01 vs omeprazole; ###p<0.001 vs omeprazole. **E)** Cell death was measured by flow cytometry of annexin V/7-AAD stained cells. Mean ± SD of three independent experiments. **p<0.01 vs control; #p<0.05 vs omeprazole. **F)** Phase contrast (x400, scale 50 µm) and TEM (x6000) images showing NAC protection from omeprazole-induced toxicity at 24 hours. Representative images of three independent experiments. **G)** HK-2 cells pretreated with NAC alone or in combination with zVAD or Fer-1 for 1 hour and stimulated with 300 µM omeprazole for 48 hours. Cell viability was assessed by the MTT assay. Mean ± SD of five independent experiments. **p<0.01 vs Omeprazole + NAC; ***p<0.001 vs omeprazole + NAC.

Figure 5. Omeprazole induces lysosomal alkalization through ROS production. A, C) HK-2 cells were stimulated with 300 µM omeprazole and lysosomal pH was measured by LysoTracker Red DND-99 (**A**) and intracellular ATP levels were measured with a Luminiscente ATP detection assay (**C**)**. B, D)** Pre-treatment with NAC preserves lysosomal pH but it does not recover intracellular ATP levels in presence of omeprazole. **A-D)** Mean ± SD of three or five independent experiments. *p<0.05 vs control, ***p<0.001 vs control; ###p<0.001 vs omeprazole.

Figure 6. Omeprazole increased the BclxL/Bax ratio and autophagy in HK-2 cells. A) HK-2 cells were stimulated with 300 μM omeprazole and Bax and BclxL protein expression was assessed by western blot. Representative Bax and BclxL western blot. Mean ± SD of three of four independent experiments. *p<0.05 vs control. **B)** BclxL/Bax ratio. Mean ± SD of three independent experiments. *p<0.05 vs control. **C)** Cells were pretreated with BclxL-BH4 peptide 1 hour before omeprazole stimulation, and cell viability was assessed by MTT. Mean ± SD of three independent experiments. **D**) Representative western blot and quantification of LC3II/LC3I ratio in HK-2 cells pretreated with different doses of 3-MA for 1 hour and stimulated with 300 μM omeprazole for 24 or 48 hours. Mean ± SD of three independent experiments. *p<0.05 vs control; #p<0.05 vs 3-MA 0 μM. **E)** Cell viability and (**F**) cytotoxicity of HK-2 cells pretreated with different doses of 3-MA for 1 hour and stimulated with 300 μM omeprazole for 48 hours. Mean ± SD of four or three independent experiments. ***p<0.001 vs control.

Figure 7. Omeprazole induces renal injury in vivo. Mice were injected daily with 40 mg/kg omeprazole for 10 or 28 days. **A)** Serum creatinine and BUN levels. **B)** Kidney mRNA expression of the renal injury marker NGAL. **C)** Cell death quantified by TUNEL staining. Representative images. Confocal microscopy. Original magnification x400. **D)** mRNA expression of Hemo-oxygenase-1 (HO-1) assessed by RT-PCR. E) Protein levels of HO-1 assessed by western blot at 28 days of omeprazole treatment. Quantification and representative image. **A-E**) Mean ± SEM of 4-5 animals per group. *p<0.05 vs control; **p<0.01 vs control; ***p<0.001 vs control.

Figure 8. Current working hypothesis. Omeprazole promotes necrotic cell death in cultured proximal tubular cells. This is associated to an early decrease in ATP levels and an early increase in mitochondrial ROS production, suggesting mitochondrial injury. ROS are instrumental in promoting necrotic cell death, which is inhibited by N-acetyl-cysteine (NAC). However, interventions over apoptosis, ferroptosis and necroptosis were not protective. Omeprazole-induced necrosis may lead to the release of cell debris that may facilitate the development of an immune response underlying the observations of acute tubulointerstitial

nephritis cases reported in omeprazole-treated patients. Additionally, omeprazole caused subclinical nephrotoxicity in mice. This is consistent with the low nephrotoxic potential of omeprazole in humans. In this regard, omeprazole nephrotoxicity may be increased by additional environmental factors, including comorbidities and concomitant medications. Among them, a frequent association is oral anticoagulants that may lead to proximal tubular cell iron overload. In cultured cells, iron overload facilitated omeprazole nephrotoxicity. The combination of these additional factors may explain why glomerular filtration rate is lost at a faster rate in patients on chronic omeprazole therapy.

Figure 1

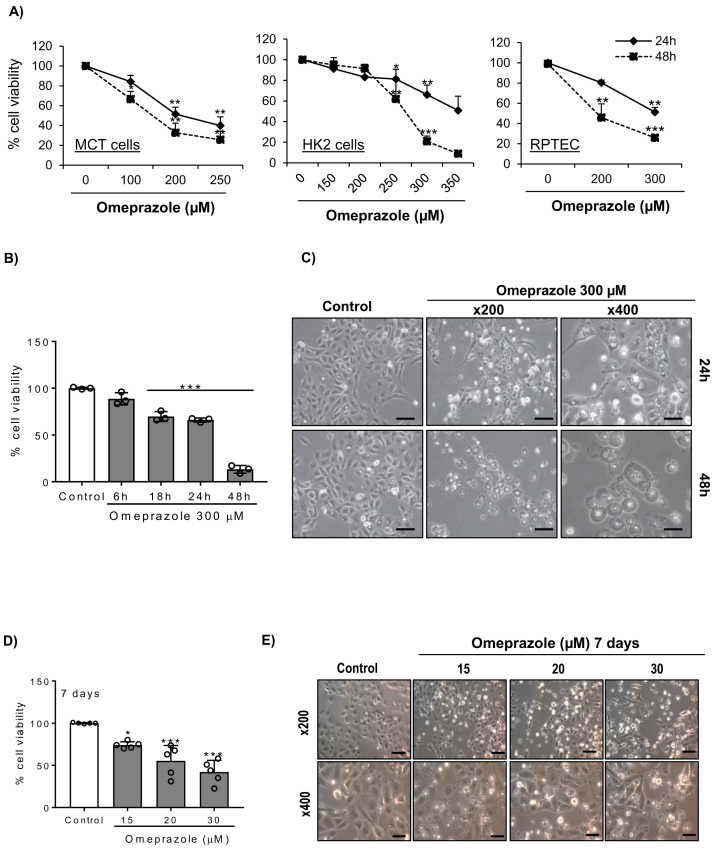

Figure 2

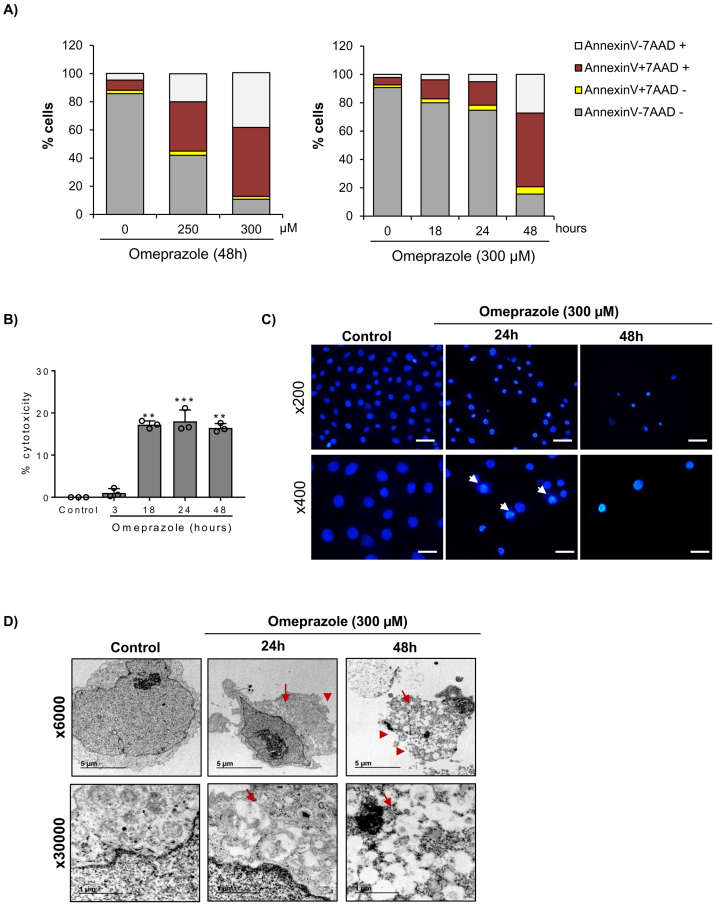

Figure 3

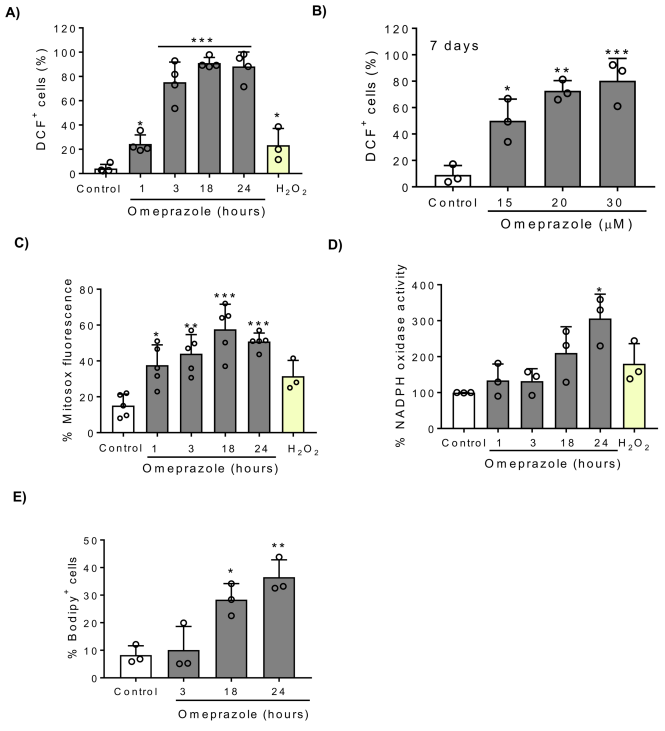
A)
DCF+ cells (%)
Control
1
3
18
24
H2O2
Omeprazole (hours)
B)
7 days
DCF+ cells (%)
Control
15
20
30
Omeprazole (μM)
C)
% Mitosox fluorescence
Control
1
3
18
24
H2O2
Omeprazole (hours)
D)
% NADPH oxidase activity
Control
1
3
18
24
H2O2
Omeprazole (hours)
E)
% Bodipy+ cells
Control
3
18
24
Omeprazole (hours)

Figure 4

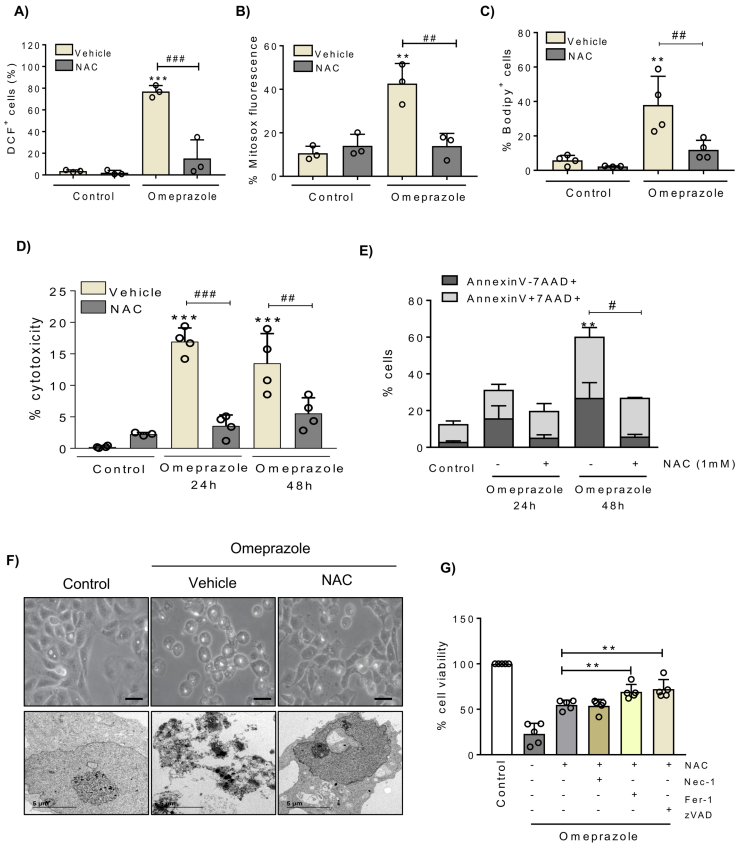
A)
B)
C)
Vehicle
NAC
DCF+ cells (%)
% Mitosox fluorescence
% Bodipy+ cells
Control
Omeprazole
D)
E)
% cytotoxicity
Omeprazole 24h
Omeprazole 48h
AnnexinV-7AAD+
AnnexinV+7AAD+
% cells
NAC (1mM)
F)
Omeprazole
Control
Vehicle
NAC
G)
% cell viability
Nec-1
Fer-1
zVAD

Figure 5

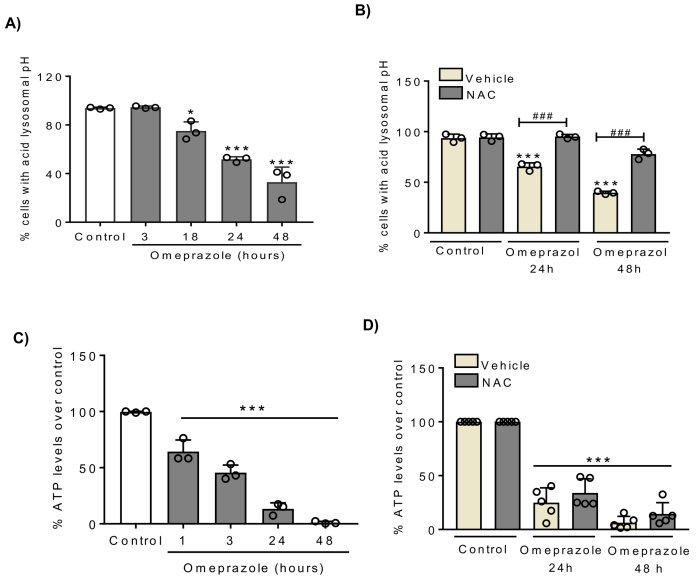

Figure 6

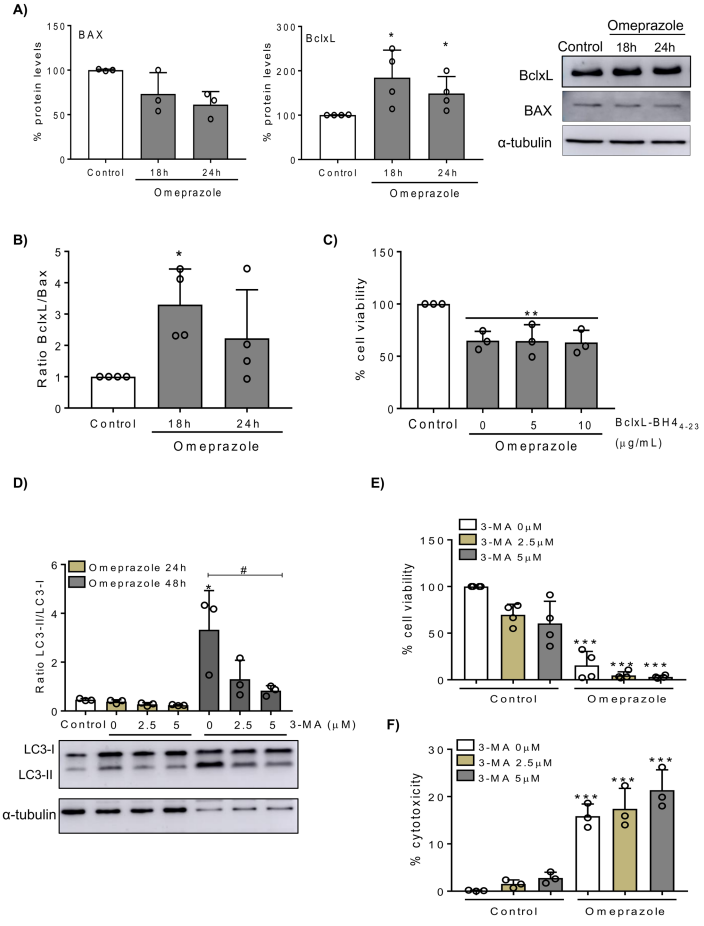

Figure 7

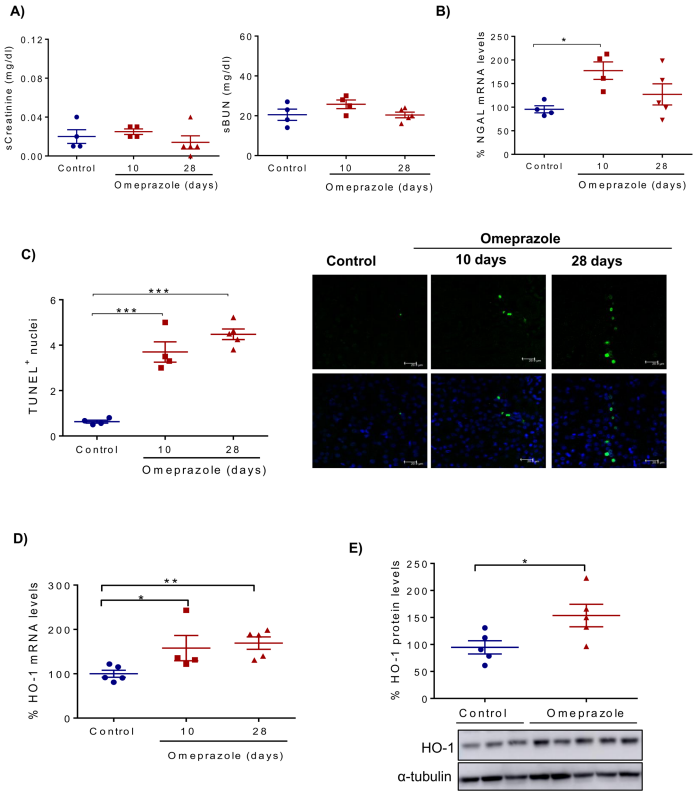
A)
sCreatinine (mg/dl)
0.12
0.08
0.04
0.00
Control
10
28
Omeprazole (days)
sBUN (mg/dl)
60
40
20
0
Control
10
28
Omeprazole (days)
B)
% NGAL mRNA levels
250
200
150
100
50
0
*
Control
10
28
Omeprazole (days)
C)
TUNEL+ nuclei
6
4
2
0
***
***
Control
10
28
Omeprazole (days)
Omeprazole
Control
10 days
28 days
D)
% HO-1 mRNA levels
300
200
100
0
**
*
Control
10
28
Omeprazole (days)
E)
% HO-1 protein levels
250
200
150
100
50
0
*
Control
Omeprazole
HO-1
α-tubulin

Figure 8

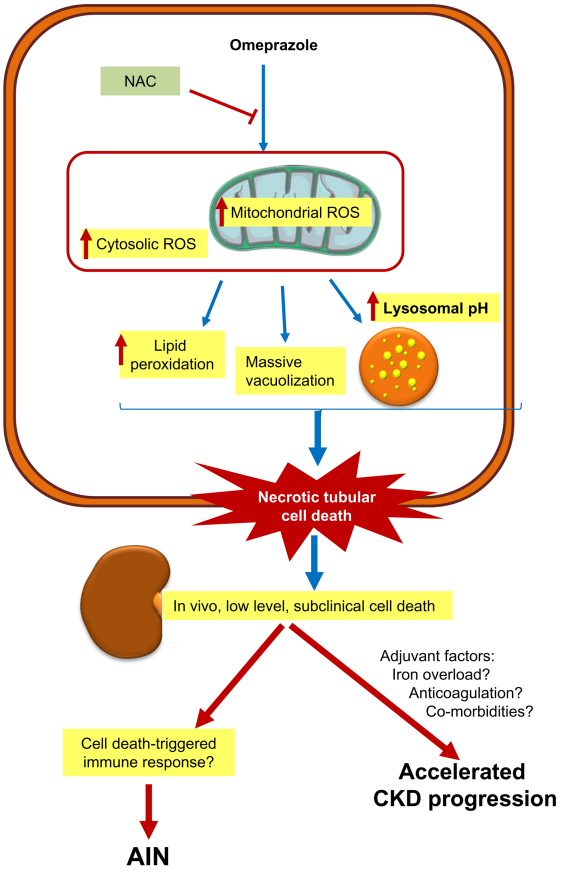

Declaration of interests

☒ The authors declare that they have no known competing financial interests or personal relationships that could have appeared to influence the work reported in this paper.

☐The authors declare the following financial interests/personal relationships which may be considered as potential competing interests: